

## Research Article



## Pharmacological Down Regulation of PRMT1 Exhibits Antagonistic Effect on Cellular Senescence Mediated by DAHP: Computational Modelling and Experimental Validation

Soniya Charles<sup>1,2</sup>, Priya Singh<sup>3</sup>, Ashwini Devi<sup>1</sup>, Amala Reddy<sup>1</sup>, Sivapatham Sundaresan<sup>2\*</sup>

<sup>1</sup> Department of Biotechnology, School of Bioengineering, SRM Institute of Science and Technology, Kattankulathur, Tamilnadu, India.

<sup>2</sup> Department of Medical Research, SRM Medical College Hospital and Research Centre, SRM University, Kattankulathur, Tamilnadu, India.

<sup>3</sup> Research Institute, SRM Institute of Science and Technology, Kattankulathur, Tamilnadu, India.

\*Corresponding author's E-mail: [ssunsr@gmail.com](mailto:ssunsr@gmail.com)

Received: 14-07-2022; Revised: 21-09-2022; Accepted: 28-09-2022; Published on: 15-10-2022.

### ABSTRACT

Metformin is intended to function as an agonist of SIRT1, a nicotinamide adenine dinucleotide (NAD<sup>+</sup>)-dependent deacetylase that mediates a number of beneficial metabolic responses. We investigated the effect of metformin in DAHP (GTPCH1 inhibitor) treated EAhy926 endothelial cells on cellular senescence. Cellular senescence was evaluated through senescence associated parameters viz., namely Beta galactosidase assay, p21 and p53 mRNA expression, nicotinamide (NAD<sup>+</sup> content), asymmetric dimethylarginine content (ADMA) content, protein arginine methylation (PRMT1) and Sirt 1 protein expression. We also performed an *in silico* investigation of the possible interactions between metformin and SIRT1 that focuses on molecular docking which revealed that metformin binds with Sirt1 and that the binding affinity of metformin with Sirt1 is prominent through docking score. Oxidative stress (OS) indices such as intracellular biopterin concentrations (tetrahydrobiopterin-BH<sub>4</sub> and dihydrobiopterin-BH<sub>2</sub>) were also determined. Metformin treatment exhibited distinct anti senescence effect in endothelial cells by downregulating the senescence markers such as beta galactosidase activity, p21 and p53 gene expression and PRMT1 protein expression while upregulating NAD<sup>+</sup> content and Sirt1 content compared to the respective controls. We postulate that metformin restores early onset of cellular senescence potentially through oxidative stress mediated cellular events in endothelial cells, one of a kind report.

**Keywords:** Cellular senescence, Protein arginine methylation, Metformin, Asymmetric dimethylarginine.

QUICK RESPONSE CODE →

DOI:

10.47583/ijpsrr.2022.v76i02.022



DOI link: <http://dx.doi.org/10.47583/ijpsrr.2022.v76i02.022>

### INTRODUCTION

GCH1 is the enzyme that slows down in the production of tetrahydrobiopterin (BH<sub>4</sub>), an important co-factor for nitric oxide synthase (NOS). Neuronal NOS (nNOS), inducible NOS (iNOS), and endothelial NOS (eNOS) are the three isoforms of nitric oxide synthase. NOS proteins form homodimers when BH<sub>4</sub> levels are sufficient, which then oxidise the substrate L-arginine to produce nitric oxide (NO), a process known as NOS coupling<sup>1</sup>. eNOS uncoupling and consequent NO shortage are caused by abnormal degradation of GTPCH1 and successive BH<sub>4</sub> insufficiency under oxidative stress state. Since DAHP affects the amounts of biopterins, it promotes eNOS uncoupling and oxidative stress (OS) hence it's been widely used to figure out the functions of BH<sub>4</sub> and DAHP mediated-GTPCH1 inhibition in pathological situations<sup>2</sup>. In particular, in the cardiovascular and cerebrovascular systems, DAHP-mediated GTPCH1 inhibition has had opposite outcomes. Recent studies on DAHP have reported, i) reactive oxygen species formation<sup>3</sup> apoptosis inhibition, and reduction in brain injury, indicating that DAHP has neuroprotective properties

against focal cerebral ischemia ii) DAHP also influences endothelial cell death by up regulating reactive oxygen species generation; and iii) in biopterin bioavailability is altered under hyperglycaemic state<sup>4</sup>.

PRMTs are classified into three categories based on their catalytic activity: type I (PRMT1 to 8) produces asymmetric dimethylarginine (ADMA) and N-monomethylarginine (NMMA); type II (PRMT5 and 9) produces symmetric dimethylarginine (SDMA) and NMMA; and type III produces monomethylarginine (MMA) (MMA). PRMTs catalyse the transfer of the methyl group from SAM to methylarginine and s-adenosylhomocysteine (SAH), which is then converted to homocysteine (HCY) in the remethylation pathway. PRMTs have also been found to methylate or impact important cell cycle and DNA damage repair regulatory proteins such Cyclin D1, p53, and p21. This shows that arginine methylation regulates the cell cycle and that SAM-dependent MTs are involved in the process<sup>5</sup>. As a result, arginine methylation can be targeted for novel medication development in diseases linked with aberrant methylation patterns, as well as aging-related disorders, by better understanding the molecular players and their associated mechanisms<sup>6</sup>.

Aging is a major factor contributing to a living organism's functional deterioration through time. The markers of ageing, such as cellular senescence and stem cell exhaustion, have recently been received much more attention directing ageing research and intervention techniques. PRMT1 and NAD<sup>+</sup> are important predictors of



cellular-senescence rate among the various variables linked to pathological senescence. Cell cycle regulation, cellular senescence, apoptotic signalling, and tissue healing have all been connected to PRMT1<sup>7</sup>. Metformin, a modest medication capable of suppressing the development of comorbidity due to ageing, has the ability to change the way we conceive about medicine in contemporary era. Metformin's ability to extend longevity has been established in animal models such as worms, mice, and rats. Metformin is thought to target a number of cellular signalling pathways involved in the progression of ageing, including inflammation, cellular survival, stress defence, autophagy, and protein synthesis<sup>8</sup>. Metformin's capacity to imitate the effects of dietary restriction by boosting adenosine monophosphate activated protein kinase (AMPK), the primary energy sensor in cells to lower energy consuming processes is one well accepted mechanism of metformin's lifetime extension. However, there is paucity of information on how metformin can slow down human cellular ageing and what processes underpin its potential effects in humans<sup>9</sup>.

Despite the research findings have shown that DAHP is linked to OS and cellular senescence, the role of DAHP in alterations in NAD<sup>+</sup> and PRMT1 is not clearly understood. In this study, we tested the effect of DAHP on cellular NAD<sup>+</sup> depletion and arginine methylation in endothelial cells in the presence or absence of metformin with an aim to better understand metformin's antagonistic effect. We have also investigated metformin's potential to improve NAD<sup>+</sup>-dependent SIRT1 activity using *insilico* docking as well as laboratory-based experimental validation. Our findings provide a first-of-its-kind structural foundation for understanding metformin's activity as a PRMT1 regulating compound<sup>10</sup>.

## MATERIALS AND METHODS

### Endothelial cell culture treatment

Human endothelial line EAhy926 was a kind gift from Dr. Suvro Chatterjee, AU-KBC Life sciences, Anna University, India. The cells were supplemented in DMEM consisting of 10% FBS (v/v). They were then treated for 24 hours with test compounds of 10mM DAHP and 0.01mM metformin (Pubchem ID: 4091). Each T25 flask was seeded with 1×10<sup>6</sup> cells per ml of medium at 37 °C in a humidified CO<sub>2</sub> incubator.

### B Galactosidase assay

The cultured endothelial cells were subjected to different experimental conditions to assess senescence related beta galactosidase activity. Endothelial cells were fixed in either 4% paraformaldehyde (PFA) and then stained for SA-βgal and quantified using flow cytometry. Growing endothelial cells were fixed and examined without SAβgal staining as a control<sup>11</sup>.

### ADMA measurement

Treated cell lysates were deproteinized using 3-kDa amicon filters<sup>12</sup>. Inertsil NH<sub>2</sub> column was used as stationary

phase and mobile phase consisted of 10mM of ammonium acetate or methanol at the flow rate of 400μl /min, 40°C using PDA detector at 260 nm. A 25μl sample was put into the HPLC system with and without spiking, and a known concentration of ADMA was used as a reference standard<sup>13</sup>.

### NAD<sup>+</sup> measurement

Deproteinized samples as previously described were injected into NH<sub>2</sub> column (250 mm × 179 4.6 mm, 5 μm Inertsil NH<sub>2</sub> column) detected using UV detector at 261 nm. Linear gradient separation was employed using mobile phase of (A) 0.05 M phosphate buffer and (B) 100% (v/v) methanol at a flow rate of 1 ml/min. The retention time of NAD<sup>+</sup> was 10.2 min and the interpretation was performed using Lab solution software<sup>14</sup>.

### BH<sub>4</sub> and BH<sub>2</sub> measurement

BH<sub>4</sub> and BH<sub>2</sub> quantification in the experimental samples were carried out using HPLC system using UV detector at wavelength of 254 nm. The deproteinized sample processed using 3kDa amicon filter was injected into ODS column (4.6x15, 5μm, 40°C at flow rate of 1ml.min. Isocratic elution program was used with 100% mobile phase A consisting of 12% methanol in 30mM KH<sub>2</sub>PO<sub>4</sub> and 0.6mM EDTA<sup>15</sup>. The sample of 20μl was injected and processed with and without spiking with known concentration of BH<sub>4</sub> and BH<sub>2</sub> as reference standard.

### p 21 and p 53 gene expression

The purity of isolated total RNA (TRIZOL reagent) was analysed spectrometrically and the RNA was used for cDNA synthesis using reverse transcriptase enzyme with Qiagen cDNA reverse transcriptase kit. The reaction mixture consisted of 3μl of total RNA, 1μL of oligo Dt18, 9μl of PCR grade water, 0.5μl of RNase inhibitor, 4 μl of reverse transcriptase buffer, 0.5μl of reverse transcriptase and 2μl of deoxynucleotide mix of total 20μl. The resultant cDNA was used for RT-PCR analysis using 10μl master mix, 2μl of synthesized cDNA and 1μl of each reverse and forward p21 and p53 primer sequences in a thermal cycler with GAPDH as internal control<sup>16</sup>.

p21: Forward 5' GACCAGCATGACAGATTC3' and Reverse 5'- TGAGACTAAGGCAGAAGATG-3'.

p53: Forward 5'TGCGTGTGGAGTATTTGGATG 3' and Reverse 5' TGGTACAGTCAGAGCCAACCTC 3'

### Sirt1 and PRMT1 protein expression

To determine the relative changes in the expression of Sirt1 and PRMT1 in the experimental samples, the immunoblot was carried out on 12% SDS gel. The separated band were transferred to nitrocellulose membrane and the membrane was blocked using blocking buffer consisting of 0.1% TBST and 5%BSA. The blocking was followed to incubation with primary antibody for 12 hrs at 4°C. The blotted membrane was then hybridized with HRP conjugated secondary antibody for 1 hr. The resultant blot was then developed using ECL kit after three washes



with TBS-T. The visualized bands were then quantified using Image Lab software<sup>17,18</sup>.

### Template selection

The amino acid sequence of human SIRT1 (Q96EB6) was obtained from the Uniport database<sup>19</sup>. The Protein Data Bank (PDB) was used to search for templates using the Basic Local Alignment Search Tool (BLAST) method. For modelling, we employed two key criteria for selecting templates: low E-value and high sequence identity<sup>20,21</sup>. A good structure's forecast is based on the % identity of at least 30-40%. Because the best picked template determines the quality of the models, the identity of the template with the query sequence is important. In this situation, we chose two templates for human SIRT1 that met the criteria for template selection.

### Homology modelling

All homology modelling data were determined by performing the programs of molecular modelling i.e. EASYMODELLER, I-TASSER<sup>22</sup> and AUTODOCK4.2 on Microsoft windows.

When the sequence information of the protein is only available, homology modelling is considered to be an important tool in 3D structure of a protein, as we observed in the case of human SIRT1 protein sequence. Therefore, we have studied the homology modeling by using various templates of human SIRT1 utilizing two different modeling platforms i.e. I-Tasser and EasyModeller. The I-Tasser which is known as Iterative Threading ASSEmblY Refinement uses the server called Local Meta-Threading Server (LOMETS) which is an online web server that uses hierarchical method for the prediction of protein three-dimensional structure whereas Easymodeller platform performs by incorporating the Modeller in the backend to generates models.

### Model validation

Various methods of model validation were used to determine the models created using homology modelling. Initially, the root mean square deviation was used to calculate the distance between the created models and the appropriate templates. Using the Yet Another Scientific Artificial Reality Application (YASARA) tool (<http://www.yasara.com/servers>), energy reduction of the created models was carried out to remove the superfluous loops in the models. The energy reduced models were validated first utilising online servers, such as the RAMPAGE online server (<http://raven.bioc.cam.ac.uk/rampage>) for ERRAT plot and Ramachandran plot validation. PROVE, an online tool, has the capacity to identify outlier amino acid residues. The Verify 3D tool was used to determine the similarity between the model generated and the amino acid sequence for analysing the three-dimensional (3D) profile. The QMEAN score was then determined using a composite scoring method in QMEAN server to determine the quality of the model developed. Low root mean square deviation (RMSD) values

between the template and the models helped us choose the best model.

### Molecular docking analysis

The interaction of biomacromolecular targets and ligands is validated using AUTODOCK4. The Lamarckian Genetic Algorithm (LGA) is utilised in this automated tool for molecular docking studies to validate the binding of Metformin with the developed model of human SIRT1. AUTODOCK (ADT) Tools1.5.6 was used to prepare the macromolecules (protein) and small molecules (ligand) for molecular docking<sup>23</sup>. The protonation of the ligand and receptors was then completed. The default Kollman charges and solvation parameters were then applied to the protein atoms. All of the ligand atoms were given Gasteiger charges. Furthermore, the docking area was chosen by constructing a grid box and spacing the target protein active site by 0.375, and the binding affinity of each ligand atom type was computed beforehand using Autogrid. Autodock4.2 was then used to simulate docking with various docking parameters based on LGA (Lamarckian Genetic Algorithm) searches, such as a maximum number of energy assessments of 25,000,000, a population size of 150, and 10 runs. Finally, the rank by energy method was used to assess the docking results of ligand and protein conformations. For further study, the ligand conformation with the lowest free binding energy was chosen as the optimal binding conformation.

## RESULTS

### Metformin restores BH<sub>4</sub>/BH<sub>2</sub> levels in endothelial cells treated with DAHP

To assess the restorative property in biopterin levels by metformin, we compared intracellular BH<sub>4</sub>/BH<sub>2</sub> concentrations in cells treated with DAHP with and without metformin. Compared to control, cells treated with DAHP significantly increased and decreased levels of BH<sub>2</sub> and BH<sub>4</sub> respectively (Fig 1). Interestingly the altered levels of BH<sub>2</sub> and BH<sub>4</sub> in cells treated with DAHP were normalised in the presence of metformin.

#### BH<sub>4</sub> and BH<sub>2</sub> measurement

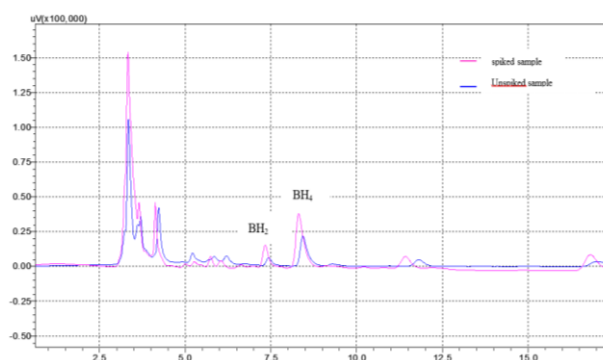


**Figure 1:** Effect of metformin restored BH<sub>4</sub> and BH<sub>2</sub> levels in DAHP- induced EAhy926 endothelial cells. HPLC analysis was performed to determine BH<sub>4</sub> and BH<sub>2</sub> levels using reference standard. Representative chromatogram of BH<sub>4</sub> and BH<sub>2</sub> with and without spiking. Endothelial cells were

treated with test compounds of 0.1mM metformin, 10Mm of DAHP independently and in combination as shown.

### Metformin downregulate $\beta$ -Gal activity in endothelial cells treated with DAHP

In DAHP-treated endothelial cells,  $\beta$ -gal activity (a senescence marker) was significantly increased by 8-fold compared to the control, whereas metformin significantly reduced beta galactosidase activity by 4 fold implying its anti-senescence activity as shown in Fig 2.

#### Beta galactosidase activity

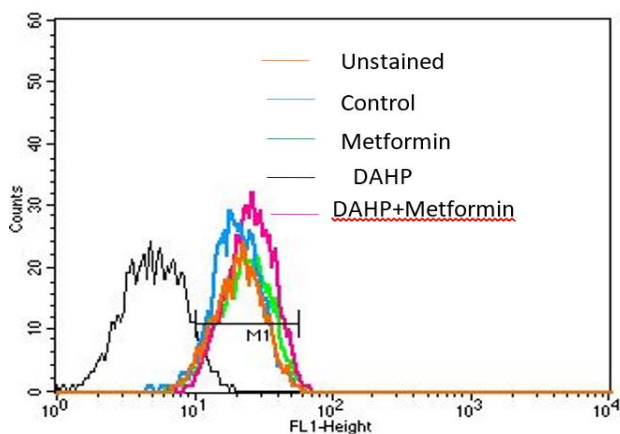


**Figure 2:** Effect of metformin reduces beta galactosidase enzyme activity under DAHP induced EAhy926 endothelial cells. Beta galactosidase activity in all the experimental conditions were quantitatively determined at 420nm.

### Metformin decreases ADMA levels

In endothelial cells, DAHP treatment increased the intracellular content of ADMA by 88% ( $p < 0.05$ ). Interestingly metformin reduced ADMA levels by 36.5% ( $p < 0.05$ ) compared to the levels seen under DAHP treatment independently as shown in Fig 3.

#### ADMA measurement

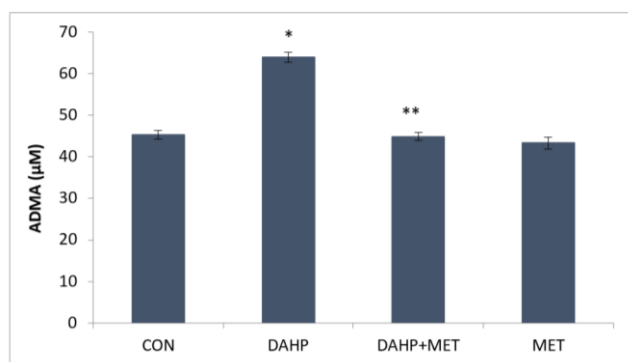


**Figure 3:** Effect of metformin on ADMA levels in DAHP-induced EAhy926 endothelial cells. HPLC analysis was performed to determine ADMA levels using reference standard. Bar graph representing ADMA levels in the experimental groups. Endothelial cells were treated with test compounds of 0.1mM metformin and 10Mm of DAHP independently and in combination as shown. Data are mean  $\pm$  SD for  $n=3$ , \* Indicates  $P < 0.05$  compared to control

and \*\*  $P < 0.05$  compared to DAHP. C – control, M – metformin, DAHP- 2,4-diamino-6-hydroxypyrimidine.

### Metformin reinforce NAD<sup>+</sup> levels:

When compared to the control, DAHP treatment lowered intracellular NAD<sup>+</sup> content significantly ( $p < 0.05$ ) in endothelial cells. Metformin mitigated the DAHP-induced inhibitory effect on NAD<sup>+</sup> concentration by increasing it significantly ( $p < 0.05$ ) as shown in Fig 4.

#### NAD<sup>+</sup> measurement

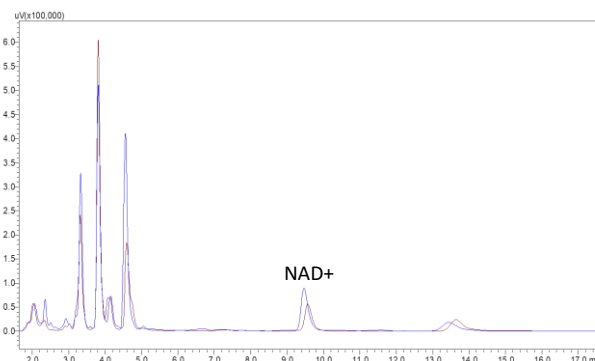


**Figure 4:** Effect of metformin restored NAD<sup>+</sup> levels to the physiological level induced by DAHP in EAhy926 cells. NAD<sup>+</sup> levels in the experimental conditions were determined using HPLC analysis using reference standard. Endothelial cells were treated with test compounds of 0.1mM metformin and 10Mm of DAHP independently and in combination. Representative HPLC chromatogram of NAD<sup>+</sup>. C – control, M – metformin, DAHP- 2,4-diamino-6-hydroxypyrimidine

### Metformin downregulate p53 and p21 expression :

There was an increase in p53 and p21 mRNA expression under DAHP treatment compared to the control (89%,  $p < 0.05$ ) and (80%,  $p < 0.05$ ), respectively. When compared to DAHP, cells treated with DAHP+ metformin significantly reduced levels of p21 and p53 mRNA levels (30% and 38% respectively,  $p < 0.05$ ) as depicted in Fig 5 (A and B).

#### RTPCR p21 and p53

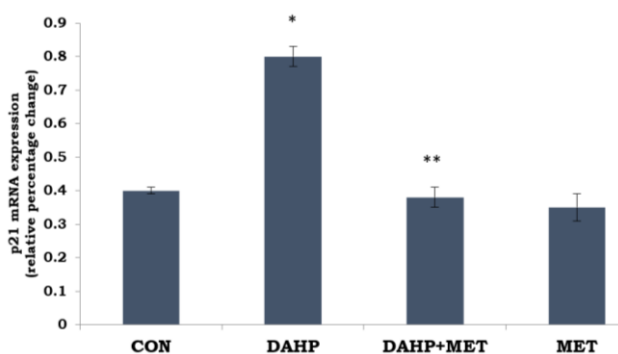


**Figure 5 A:** Effect of metformin reduces p21 mRNA levels under DAHP induced EAhy926 endothelial cells. Endothelial cells were treated with test compounds of 0.1Mm metformin, and 10mM of DAHP independently and in combination as shown. Data are mean  $\pm$  SD for  $n=3$ , \* Indicates  $P < 0.05$  compared to control and \*\*  $P < 0.05$

compared to DAHP. C – control, M –metformin, DAHP- 2,4-diamino-6-hydroxypyrimidine

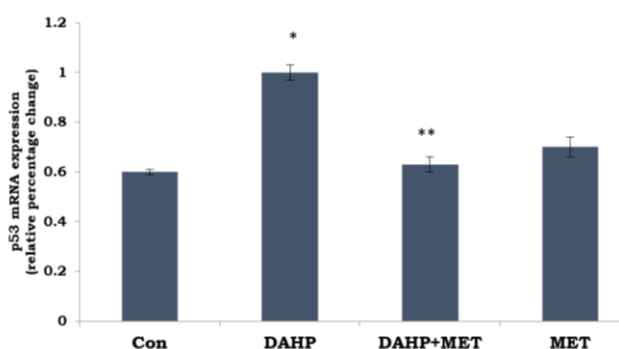


**Fig 5B:** Effect of metformin downregulates p53 mRNA levels under DAHP induced EAhy926 endothelial cells. Endothelial cells were treated with test compounds of 0.1Mm metformin and 10mM of DAHP independently and in combination as shown. Data are mean  $\pm$  SD for n=3, \* Indicates  $P < 0.05$  compared to control and \*\*  $P < 0.05$  compared to DAHP. C – control, M –metformin, DAHP- 2,4-diamino-6-hydroxypyrimidine.

#### Sirt1 and PRMT1 protein expression by western blot

Compared to control cells, cells treated with DAHP exhibited a significant decrease in Sirt1 protein levels (45%,  $p \leq 0.05$ ) and significant increase in PRMT1 protein levels (52%,  $p \leq 0.05$ ) as shown in Fig 7. Interestingly, the alterations induced by DAHP were significantly ( $p \leq 0.05$ ) normalised and restored in cells treated with metformin as depicted in Fig 6.

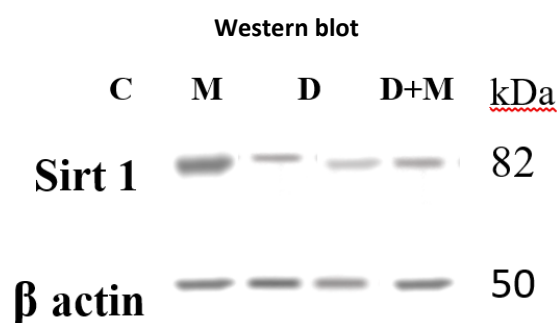


**Figure 6:** Effect of metformin on Sirt1 protein expression under DAHP induced EAhy926 endothelial cells. (A) Western blot analysis presents an increasing tendency in Sirt 1 expression in the DAHP+MET group, as compared with the respective controls. C – control, M –metformin, DAHP- 2,4-diamino-6-hydroxypyrimidine

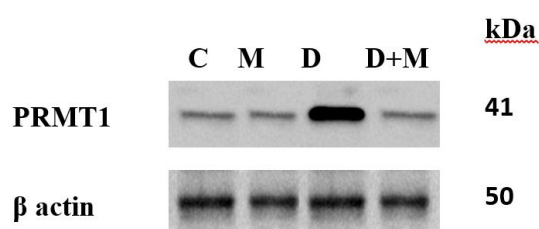


**Figure 7:** Effect of metformin on PRMT1 protein expression under DAHP induced EAhy926 endothelial cells. (A)

Western blot analysis presents an decreasing tendency in PRMT11 expression in the DAHP+MET group, as compared with the respective controls. C – control, M –metformin, DAHP- 2,4-diamino-6-hydroxypyrimidine.

#### Template selection

The templates for human SIRT1 protein structure modelling were identified using the Basic Local Alignment Search Tool (BLAST) search technique against the PDB (Protein Data Bank). SIRT1 (PDB IDs: 5BTR, 4ZZH) was found as a suitable modelling template through a BLAST search. The top templates were chosen based on the routine selection criteria, which required sequence identity to be greater than 40% and query coverage to be greater than 70%. Fig 8 depicts the sequence alignment between the chosen template (5BTR) and human SIRT1. The chosen template has query coverage of greater than 50% and sequence identity of 90-100 %.

#### Homology model generation and validation

The homology models were created with the help of two separate modelling platforms: I-TASSER and Easymodeller 4.0.

Following model generation, the resulting models were validated using the RMSD value between the template and the model, as well as other validation servers. The model was validated using the Ramachandran plot<sup>24</sup>, ERRAT plot, QMEAN score, Verify3D, PROVE, and ProSA Z-score servers. Model07 (EasyModeller) and model01 (Human SIRT1) were chosen as the best human SIRT1 models (I-TASSER). The validation statistics data of the selected human SIRT1 models are shown in Table.1.

The produced model 07's DOPE score in human SIRT1 was -49818.058, and the RMSD value with the template was 0.851. The majority of residues (96.8%) are found in the favourable and authorised regions, with an ERRAT plot-based quality factor score of 32.707 (Fig 9 B). Model 01 revealed 75.3 percent favourable residues and 16.2% acceptable residues. The model 01's ERRAT score was 89.959, which is a good value. The model 01's PROVE value is 7.2, and the model 07's ProSA Z-score is -3.3. The model 07 had a QMEAN core of -7.13, whereas the model 01 had a score of -7.90. In the 3D/1D profile, 64.52 percent of the residues scored 0.2 in the verify 3D validation score for model 01 similarly, 56.22 of the residues in model 07 had a score of 0.2. These statistical model validations revealed that the models created were suitable and viable for molecular docking research.

#### Molecular docking analysis

Metformin was docked with the human SIRT1 models that were created. The macromolecule (protein) was docked with the tiny molecule using the Autodock 4.2 tool. The human SIRT1 structure was individual docked with the selected ligand Metformin. The docking score depicted that confirmations highlighted in yellow formed strong hydrogen bonding interaction with the SIRT1 active site pocket. Metformin showed strong hydrogen bonding with

active site residue SER682, PRO688 with the dock score - 5.34. These docking interactions suggested that these selected ligands exhibit effective inhibition effect to down regulate the enzymatic activity of methyl transferases activity that can be used effectively against myocardial

related disorders and type2 diabetes treatment and plausibly could have clinical benefits. Table 2 shows the molecular docking of human SIRT1 predicted model 07 with Metformin. From docking, the predicted binding configuration of Metformin bound to human SIRT1.

### Homology model generation and validation

**Table 1:** Represents Ramachandran plot values and generated model of SIRT1 validation score values

Model	RMSD (Å)	Ramachandran plot		DOPE Score	ERRAT	ProSA Z-score	PROVE	QMEAN score	Verify 3D%
		Number of residues in favored region	Number of residues in allowed region						
1	0.459	576 (75.3%)	121 (16.2%)	NA	89.959	NA	7.2	-7.90	64.52
7	0.851	684 (91.8%)	37 (5.0%)	-49818.058	32.707	-3.3	NA	-7.13	56.22

**Table 2:** Predicted interaction conformation of Metformin with human SIRT11 structure. The hydrogen bond formation between the residuesSER682, PRO688 and ligand (yellow lines) and side chain hydrophobic residues

Protein	Ligand	Total AUTODOCK Score	Number of H-bonds	Residues involved in H-bonding with ligand	Residues involved in hydrophobic bonds formation
SIRT1	Metformin	-5.34	2	SER682, PRO688	PHE698, ASP707, PRO271, VAL285, GLY385

### DISCUSSION

We observed four senescence-related events, four cellular function variables as OS indicators, and a first-in-class computational research to detangle metformin's probable binding mechanisms to the SIRT1 enzyme while DAHP increases cellular senescence it appears that metformin offers an antagonistic impact against cellular senescence. In our study, metformin inhibited the onset of cellular senescence induced by DAHP in endothelial cells, as evident from decreased intracellular beta galactosidase activity, ADMA depletion, NAD<sup>+</sup> accumulation, decreased p21, p53 gene expression, increased Sirt1 expression, and decreased PRMT1 protein expression<sup>27</sup>. Despite the fact that metformin is predicted to interact with SIRT1's catalytic domain, the present study shows that it can improve SIRT1's catalytic efficiency. Metformin has previously been proven to serve as a true SIRT1 agonist to prevent Th17 cell development when taken at low millimolar dosages incapable of activating the energy-sensing AMPK/mTOR pathway, similar to well-known SIRT1 activators such as resveratrol and SRT1720. Several cellular processes have been found to have an antagonistic effect against cellular senescence, including GTPCH1 inhibition, beta galactosidase activity, NAD<sup>+</sup> depletion, p21, p53 depletion, and Sirt1 accumulation<sup>28</sup>. It appears that metformin has a regulatory role in cellular senescence in a pathogenic situation based on our observations and conclusions, because DAHP promulgates cellular senescence<sup>29</sup>.

DAHP enhances OS and affects several senescence-related processes and this has been widely reported<sup>18</sup>. DAHP influences OS, mitochondrial redox, and metabolic activity, as well as eNOS uncoupling, through altering senescence mechanisms via peroxynitrite synthesis, antioxidant

depletion, ATP generation, PARP, and DNA damage. Metformin-induced increased NO bioactivity is also consistent with previous studies that demonstrated metformin improving endothelial vascular function via increasing AMPK-dependent, hsp90-mediated eNOS activation<sup>30</sup>. DAHP decreased vasorelaxation and eNOS uncoupling-induced heart damage due to BH<sub>4</sub> deficiency. Furthermore, DAHP impaired cardiac contractile performance by accumulating reactive oxygen species in mitochondria, and cardiac ageing was associated to diminished mitochondrial function and myocardial contraction<sup>31</sup>.

Metformin has been shown to improve endothelial function and protect the macro- and microvasculature in diabetic patients via mechanisms unrelated to its hypoglycemia effects<sup>32</sup>. As a result of these findings in microvascular endothelial cells, Sirt1 appears to be a crucial target for metformin's endothelium-protective effects<sup>33</sup>. Sirt1 has been reported to work as a deacetylase for a number of transcription factors, including p53, and therefore could regulate cell differentiation, senescence, and survival in response to cellular stress. Oxidative stress-induced downregulation of Sirt1 caused eNOS acetylation and endothelial dysfunction. Furthermore, as evidenced by increased β-galactosidase activity in HUVECs, a decrease in SIRT1 expression caused by hyperglycemia/ROS, as well as the Sirt1 inhibitor sirtinol, accelerates vascular senescence<sup>34</sup>. When compared to controls, metformin treatment attenuated the effects of DAHP-induced endothelial dysfunction-mediated cellular senescence, as demonstrated by decreased levels of senescent markers such as p21, p53 gene expression, decreased β-galactosidase activity, and increased levels of Sirt 1 protein expression<sup>35</sup>.



With substantial docking scores of -5.34, metformin has a greater binding affinity for Sirt1's active site. Metformin showed great potency in terms of cell cycle arrest and PRMT1 transcript decrease, as well as two hydrogen bonding interactions with SER682, PRO688 with a high docking score. Similarly, docked confirmation of the ligands metformin and Sirt1 revealed that the ligands made significant bonded and non-bonded interactions with the residues of the target enzyme Sirt1, resulting in higher docking scores – 5.34. Sirt1, metformin, and SER682, PRO688, and hydrophobic interactions with PHE698, ASP707, PRO271, VAL285 and GLY385. In terms of Sirt1 transcripts, ADMA concentration, and p21, p53 expression in endothelial cells, metformin had a higher docking score than the most active molecule, indicating that the antagonistic effect of the most active drug could be due to mechanisms other than PRMT1 inhibition<sup>36</sup>. We performed HPLC measurement of intracellular NAD<sup>+</sup> and ADMA levels to further confirm our findings on senescence. The combined treatment increased NAD<sup>+</sup> levels by 72 % and reduced ADMA by 34 %, while DAHP alone lowered NAD<sup>+</sup> levels by 46 % and reduced ADMA by 74 %.

Several studies have found that physiological NAD<sup>+</sup> levels are important in slowing down the ageing process. For instance, NAD<sup>+</sup> depletion, which is mostly induced by OS, has an impact on the activities of NAD<sup>+</sup>-dependent enzymes including PARP and sirtuins<sup>37</sup>. Because PARP controls oxidative DNA damage repair, cell cycle progression, cell survival, and genomic integrity, normal PARP activation is a physiological response to NAD<sup>+</sup> depletion<sup>38</sup>. However in pathological conditions, PARP over-activation depletes NAD<sup>+</sup> and reduces cell viability. In our study, metformin caused significant NAD<sup>+</sup> modulation, with levels of NAD<sup>+</sup> increasing by more than 50%. This could be one of the main reasons for the decreased beta galactosidase activity in cells treated with metformin<sup>39</sup>. Second, PARP-mediated NAD<sup>+</sup> depletion depletes the internal ATP pool, allowing autophagy molecules to be released and cell death to proceed. Finally, sirtuins play a role in ageing, senescence, and apoptosis. For proper sirtuin1 (SIRT1) deacetylase activity, physiological NAD<sup>+</sup> content is essential. Hyper-activated PARP-mediated NAD<sup>+</sup> depletion affects SIRT1 activity in pathological circumstances, resulting in hyper-activation of apoptotic effectors such as p21 and p53, causing cells to become over-sensitized to apoptosis. NAD<sup>+</sup> deficiency has an indirect effect on cellular GSH, whereas increased reactive oxygen species have a direct effect on GSH concentration<sup>40</sup>. Low levels of NAD<sup>+</sup> and GSH impeded energy metabolism, anti-oxidative, and anti-apoptotic properties, according to an in vitro experiment<sup>41</sup>. Our new findings imply that a sufficient amount of NAD<sup>+</sup> is required to maintain SIRT1 active, which aids in the repair of OS-induced cellular damage and prevents apoptosis. As a result of our findings, which reveal a considerable drop in intracellular NAD<sup>+</sup> level in DAHP treated cells that is recovered by metformin treatment, it is probable that the intracellular OS response mechanisms are repaired, potentiating the antisenescence impact<sup>42</sup>.

Sirt1 and PRMT1 both reduce GTPCH1 activity because GTPCH1 is found in eNOS and caveolin1<sup>43</sup>. DAHP has been shown to closely regulate OS via Sirt1 and caveolin1 protein-protein interactions<sup>44</sup>. These findings suggest that the appropriate intracellular functioning of GTPCH1, Sirt1, and PRMT1 are interdependent. In this context, it's worth examining if metformin modulates PRMT1 via Sirt1 in the DAHP-induced endothelial dysfunction state. In a DAHP-induced scenario, metformin raised intracellular NAD<sup>+</sup> protein levels while decreasing PRMT1 protein concentrations, as per immunoblot analyses of Sirt1 and PRMT1<sup>45</sup>. As previously stated, it is possible that PRMT1 hypermethylation induces senescence. A recent study that found consistent cellular senescence and enhanced DNA damage in PRMT1-KD cells, as well as PRMT1 deletion in MEF cells, led to spontaneous DNA damage, supports our conclusion that metformin could regulate cellular senescence<sup>46</sup>. In the DAHP groups, we detected p53 and p21 induction at the RNA level. The gene expression of p53 and p21, on the other hand, was reduced in a metformin-treated state<sup>47</sup>. The expression of p21, p53 targets, and cyclin-dependent kinase inhibitor determines cell senescence. These findings confirm the importance of p53 and p21 in triggering senescence genes in endothelial cells during DAHP-induced senescence<sup>48</sup>. Endothelial dysfunction is a common complication of diabetes and is significantly linked to the risk of cardiovascular disease. Metformin treatment was linked to lower levels of sVCAM-1 in the blood, as well as improved endothelial regulation of haemostasis, leucocyte adhesion, and fibrinolysis<sup>49</sup>. Metformin's effects on endothelial function were largely unrelated to reductions in hyperglycemia, insulin dosage, or BMI, implying that metformin had direct effects on the endothelium<sup>50</sup>.

Our research does have certain limitations. Despite the fact that pharmacological inhibition of GTPCH1 has clearly demonstrated, GTPCH1's role in senescence, future siRNA-based research will shed light on the effect of GTPCH1 inhibition or BH<sub>4</sub> depletion on cell senescence. There is a scarcity of data on physiological reactive oxygen and nitrogen species produced by superoxide/peroxynitrite inhibitors or reactive oxygen species scavengers. GTPCH1 inhibition, metformin treatment, altered redox signalling, and senescence all intersect, providing an opportunity to learn more about this notion.

## CONCLUSION

While endothelial cells treated with DAHP exhibits several stress signals alteration and increased senescence, metformin boosts NAD<sup>+</sup> content, deteriorates beta galactosidase activity, lowers ADMA content, downregulate gene expression of p21, p53 and upregulate Sirt1 protein level and reduces PRMT1 protein levels with a net result of its antisenescent activity.

**Acknowledgement:** The current study was partly supported by the research grant from Selective Excellence Initiative Scheme- SRMIST, Kattankulathur, Chennai, India. We thank Dr. Jesu Arockiaraj, Research Institute, SRM IST,



Kattankulathur, Chennai for providing the lab space for conducting all the experiments.

## REFERENCES

- Thony B, Auerbach G, Blau N. Tetrahydrobiopterin biosynthesis, regeneration and functions. *Biochemical Journal* 2000; 347(1):1-16. Doi: 10.1042/bj3470001; PMID: 10727395.
- Yang YM, Huang A, Kaley G, Sun D. eNOS uncoupling and endothelial dysfunction in aged vessels. *American Journal of Physiology-Heart and Circulatory Physiology* 2009; 297(5), H1829-H1836. Doi: 10.1152/ajpheart.00230; PMID: 19767531.
- Incalza MA, D'Oria R, Natalicchio A, Perrini S, Laviola L, Giorgino F. Oxidative stress and reactive oxygen species in endothelial dysfunction associated with cardiovascular and metabolic diseases. *Vascular pharmacology* 2018; 100:1-19. Doi: 10.1016/j.vph.2017.05.005; PMID:28579545
- Carnicer R, Duglan D, Ziberna K, Recalde A, Reilly S, Simon JN, Casadei B. BH<sub>4</sub> Increases nNOS Activity and Preserves Left Ventricular Function in Diabetes. *Circulation Research* 2021; 128(5): 585-601. Doi: 10.1161/CIRCRESAHA.120.316656; PMID: 33494625.
- Kim JH, Yoo BC, Yang WS, Kim E, Hong S, Cho JY. The role of protein arginine methyltransferases in inflammatory responses. *Mediators of Inflammation* 2016; Doi: 10.1155/2016/4028353; PMID: 27041824.
- Blanc RS, Richard S. Arginine methylation: the coming of age. *Molecular cell* 2017; 65(1): 8-24. Doi: 10.1016/j.molcel.2016.11.003; PMID: 28061334.
- Lai Y, Li J, Li X, Zou C. Lipopolysaccharide modulates p300 and Sirt1 to promote PRMT1 stability via an SCFFbx17-recognized acetyldegron. *Journal of cell science* 2017; 130(20): 3578-3587. Doi: 10.1242/jcs.206904; PMID: 288830.
- Rena G, Hardie DG, Pearson ER. The mechanisms of action of metformin. *Diabetologia* 2017; 60(9): 1577-1585. Doi: 10.1007/s00125-017-4342-z; PMID: 28776086.
- Choi SY, Lee C, Heo MJ, Choi YM, An S, Bae S, Jung JH. Metformin ameliorates animal models of dermatitis. *Inflammopharmacology* 2020; 28(5): 1293-1300. Doi: 10.1007/s00125-017-4342-z; PMID: 28776086.
- Bharath LP, Agrawal M, McCambridge G, Nicholas DA, Hasturk H, Liu J, Nikolajczyk BS. Metformin enhances autophagy and normalizes mitochondrial function to alleviate aging-associated inflammation. *Cell metabolism* 2020; 32(1): 44-55. Doi: 10.1016/j.cmet.2020.04.015; PMID: 32402267.
- Mockli N, Auerbach D. Quantitative  $\beta$ -galactosidase assay suitable for high-throughput applications in the yeast two-hybrid system. *Biotechniques* 2004; 36(5): 872-876. Doi: 10.2144/04365PT03; PMID: 15152608.
- Blackwell S, O'Reilly DSJ, Talwar DK. HPLC analysis of asymmetric dimethylarginine (ADMA) and related arginine metabolites in human plasma using a novel non-endogenous internal standard. *Clinica Chimica Acta* 2009; 401(1-2): 14-19. Doi: 10.1016/j.cca.2008.10.032; PMID: 19027728.
- Teerlink T. HPLC analysis of ADMA and other methylated L-arginine analogs in biological fluids. *Journal of Chromatography B* 2007; 851(1-2): 21-29. Doi: 10.1016/j.cca.2008.10.032; PMID: 19027728.
- Yoshino J, Mills KF, Yoon MJ, Imai SI. Nicotinamide mononucleotide, a key NAD<sup>+</sup> intermediate, treats the pathophysiology of diet-and age-induced diabetes in mice. *Cell metabolism* 2011; 14(4): 528-536. Doi: 10.1016/j.cmet.2011.08.014; PMID: 21982712.
- Wu HE, Baumgardt SL, Fang J, Paterson M, Liu Y, Du J, Ge ZD. Cardiomyocyte GTP cyclohydrolase 1 protects the heart against diabetic cardiomyopathy. *Scientific reports* 2016; 6(1): 1-14. Doi: 10.1038/srep27925; PMID: 27295516.
- Orchel A, Molin I, Dzierzewicz Z, Latocha M, Weglarz L, Wilczok T. Quantification of P21Gene expression in Caco-2 cells treated with sodium butyrate using real-time reverse transcription-PCR (RT-PCR) assay. *Acta poloniae pharmaceutica* 2003;60(2): 103-105.PMID:13678314.
- Kilic U, Gok O, Erenberk U, Dundaroz MR, Torun E, Kucukardali Y, Dundar T. A remarkable age-related increase in SIRT1 protein expression against oxidative stress in elderly: SIRT1 gene variants and longevity in human. *PloS one* 2015; 10(3): e0117954. Doi: 10.1371/journal.pone.0117954; PMID: 25785999.
- Herrmann F, Lee J, Bedford MT, Fackelmayer FO. Dynamics of human protein arginine methyltransferase 1 (PRMT1) in vivo. *Journal of Biological Chemistry* 2005; 280(45): 38005-38010. Doi: 10.1074/jbc.M502458200; PMID: 16159886.
- Wang W, Kramer PM, Yang S, Pereira MA, Tao L. Reversed-phase high-performance liquid chromatography procedure for the simultaneous determination of S-adenosyl-L-methionine and S-adenosyl-L-homocysteine in mouse liver and the effect of methionine on their concentrations. *Journal of Chromatography B: Biomedical Sciences and Applications* 2001; 762(1): 59-65. Doi: 10.1016/s0378-4347(01)00341-3; PMID: 11589459.
- Dallavilla T, Bertelli M, Morresi A, Bushati V, Stuppia L, Beccari T, Marceddu G. Bioinformatic analysis indicates that SARS-CoV-2 is unrelated to known artificial coronaviruses. *Eur Rev Med Pharmacol Sci* 2020; 24(8): 4558-4564. Doi: 10.26355/eurrev\_202004\_21041; PMID: 32373995.
- Altschul SF, Gish W, Miller W, Myers EW, Lipman DJ. Basic local alignment search tool. *Journal of molecular biology* 1990; 215(3): 403-410. Doi: 10.1016/S0022-2836(05)80360-2; PMID: 2231712.
- Roy A, Kucukural A, Zhang Y. I-TASSER: a unified platform for automated protein structure and function prediction. *Nature protocols* 2010; 5(4): 725-738. Doi: 10.1038/nprot.2010.5; PMID: 20360767.
- Sahoo M, Jena L, Rath SN, Kumar S. Identification of suitable natural inhibitor against influenza A (H1N1) neuraminidase protein by molecular docking. *Genomics & informatics* 2016; 14(3): 96. Doi: 10.5808/GI.2016.14.3.96; PMID: 27729839.
- Carugo O, Djinović-Carugo K. Half a century of Ramachandran plots. *Acta Crystallographica Section D: Biological Crystallography* 2013; 69(8): 1333-1341. Doi: 10.1107/S090744491301158X; PMID: 23897457.
- Jirouskova Z, Varekova RS, Vanek J, Koca J. Electronegativity equalization method: parameterization and validation for organic molecules using the Merz-Kollman-Singh charge distribution scheme. *Journal of computational chemistry* 2009; 30(7): 1174-1178. Doi: 10.1002/jcc.21142; PMID: 18988249.
- Gurcu S, Girgin G, Yorulmaz G, Kılıçarslan B, Efe B, Baydar T. Neopterin and biopterin levels and tryptophan degradation in patients with diabetes. *Scientific reports* 2020; 10(1): 1-8. Doi: 10.1038/s41598-020-74183-w; PMID: 33046801.
- Ye J, Luo D, Xu X, Sun M, Su X, Tian Z, Guan Q. Metformin improves fertility in obese males by alleviating oxidative stress-induced blood-testis barrier damage. *Oxidative medicine and cellular longevity* 2019; Doi: 10.1155/2019/9151067; PMID: 31583050.
- Hwang JW, Yao H, Caito S, Sundar IK, Rahman I. Redox regulation of SIRT1 in inflammation and cellular senescence. *Free Radical Biology and Medicine* 2013; 61: 95-110. Doi: 10.1016/j.freeradbiomed.2013.03.015; PMID: 23542362.
- Charles S, Raj V, Ramasamy M, Ilango K, Arockiaraj J, Murugesan S, Mala K. Pharmacological inhibition of guanosine triphosphate cyclohydrolase1 elevates tyrosine phosphorylation of caveolin1 and cellular senescence. *European journal of pharmacology* 2019; 848: 1-10. Doi: 10.1016/j.ejphar.2019.01.036; PMID: 30690003.
- Kurz DJ, Decary S, Hong Y, Erusalimsky JD. Senescence-associated (beta)-galactosidase reflects an increase in lysosomal mass during





- replicative ageing of human endothelial cells. *Journal of cell science* 2000; 113(20): 3613-3622. Doi: 10.1242/jcs.113.20.3613; PMID: 11017877.
31. Das A, Huang GX, Bonkowski MS, Longchamp A, Li C, Schultz MB, Sinclair DA. Impairment of an endothelial NAD<sup>+</sup>-H2S signaling network is a reversible cause of vascular aging. *Cell* 2018; 173(1): 74-89. Doi: 10.1016/j.cell.2018.02.008; PMID: 29570999.
  32. Kim GD, Park S. Effects of Cudratriacuspida on anti-senescence in high glucose-treated endothelial cells via the Akt/p53/p21 pathway. *Food Science & Nutrition* 2020; 8(11): 5999-6006. Doi: 10.1002/fsn3.1885; PMID: 33282251.
  33. Wu Q, Hu Y, Jiang M, Wang F, Gong G. Effect of autophagy regulated by Sirt1/FoxO1 pathway on the release of factors promoting thrombosis from vascular endothelial cells. *International journal of molecular sciences* 2019; 20(17): 4132. Doi: 10.3390/ijms20174132; PMID: 31450612.
  34. Wu Y, Ding Y, Ramprasath T, Zou MH. Oxidative stress, GTPCH1, and endothelial nitric oxide synthase uncoupling in hypertension. *Antioxidants & redox signaling* 2021; 34(9): 750-764. Doi: 10.1089/ars.2020.8112; PMID: 32363908.
  35. Karbach S, Wenzel P, Waisman A, Munzel T, Daiber A. eNOS uncoupling in cardiovascular diseases-the role of oxidative stress and inflammation. *Current pharmaceutical design* 2014; 20(22): 3579-3594. Doi: 10.2174/13816128113196660748; PMID: 24180381.
  36. Moens, AL, Kass DA. Tetrahydrobiopterin and cardiovascular disease. *Arteriosclerosis, thrombosis, and vascular biology* 2006; 26(11): 2439-2444. Doi: 10.1161/01.ATV.0000243924.00970.cb; PMID: 16946131.
  37. Niu C, Chen Z, Kim KT, Sun J, Xue M, Chen G, Li X. Metformin alleviates hyperglycemia-induced endothelial impairment by downregulating autophagy via the Hedgehog pathway. *Autophagy* 2019; 15(5): 843-870. Doi: 10.1080/15548627.2019.1569913; PMID: 30653446.
  38. Fen-fang H, Xiao-yu L, Liu W, Lv S, Shu-jin H, Kuang HB, Shu-long Y. Roles of eNOS in atherosclerosis treatment. *Inflammation Research* 2019; 68(6): 429-441. Doi: 10.1007/s00011-019-01229-9; PMID: 30937466.
  39. Gielis JF, Lin JY, Winkler K, Van Schil PE, Schmidt HH, Moens AL. Pathogenetic role of eNOS uncoupling in cardiopulmonary disorders. *Free Radical Biology and Medicine* 2011; 50(7): 765-776. Doi: 10.1016/j.freeradbiomed.2010.12.018; PMID: 21172428.
  40. Fisher JJ, Bartho LA, Perkins AV, Holland OJ. Placental mitochondria and reactive oxygen species in the physiology and pathophysiology of pregnancy. *Clinical and Experimental Pharmacology and Physiology* 2020; 47(1): 176-184. Doi: 10.1111/1440-1681.13172; PMID: 31469913.
  41. Ikonomidis I, Pavlidis G, Thymis J, Birba D, Kalogeris A, Kousathana F, Lambadiari V. Effects of glucagon-like peptide-1 receptor agonists, sodium-glucose cotransporter-2 inhibitors, and their combination on endothelial glycocalyx, arterial function, and myocardial work index in patients with type 2 diabetes mellitus after 12-month treatment. *Journal of the American Heart Association* 2020; 9(9): e015716. Doi: 10.1161/JAHA.119.015716; PMID: 32326806.
  42. Jiating L, Buyun J, Yinchang Z. Role of metformin on osteoblast differentiation in type 2 diabetes. *BioMed research international* 2019; Doi: 10.1155/2019/9203934; PMID: 31886264.
  43. Ham YH, Jason Chan KK, Chan W. Thioproline serves as an efficient antioxidant protecting human cells from oxidative stress and improves cell viability. *Chemical research in toxicology* 2020; 33(7): 1815-1821. Doi: 10.1021/acs.chemrestox.0c00055; PMID: 32299210.
  44. Ke Y, Li D, Zhao M, Liu C, Liu J, Zeng A, Hong H. Gut flora-dependent metabolite Trimethylamine-N-oxide accelerates endothelial cell senescence and vascular aging through oxidative stress. *Free Radical Biology and Medicine* 2018; 116: 88-100. Doi: 10.1016/j.freeradbiomed.2018.01.007; PMID: 29325896.
  45. Covarrubias AJ, Perrone R, Grozio A., & Verdin, E. NAD<sup>+</sup> metabolism and its roles in cellular processes during ageing. *Nature Reviews Molecular Cell Biology* 2021; 22(2): 119-141. Doi: 10.1038/s41580-020-00313-x; PMID: 33353981.
  46. Yaku K, Okabe K, Nakagawa T. NAD metabolism: Implications in aging and longevity. *Ageing research reviews* 2018; 47: 1-17. Doi: 10.1016/j.arr.2018.05.006; PMID: 29883761.
  47. Martín-Guerrero SM, Casado P, Hijazi M, Rajeev V, Plaza-Díaz J, Abadía-Molina F, Martín-Oliva D. PARP-1 activation after oxidative insult promotes energy stress-dependent phosphorylation of YAP1 and reduces cell viability. *Biochemical Journal* 2020; 477(23): 4491-4513. Doi: 10.1042/BCJ20200525; PMID: 33146386.
  48. Kahlenberg JM, Dubyak GR. Mechanisms of caspase-1 activation by P2X7 receptor-mediated K<sup>+</sup> release. *American Journal of Physiology-Cell Physiology* 2004; 286(5): C1100-C1108. Doi: 10.1042/BCJ20200525; PMID: 33146386.
  49. Hong Q, Zhang L, Das B, Li Z, Liu B, Cai G, Lee, K. Increased podocyte Sirtuin-1 function attenuates diabetic kidney injury. *Kidney international* 2018; 93(6): 1330-1343. Doi: 10.1016/j.kint.2017.12.008; PMID: 29477240.
  50. Das T, Paino D, Manoharan A, Farrell J, Whiteley G, Kriel FH, Manos J. Conditions under which glutathione disrupts the biofilms and improves antibiotic efficacy of both ESKAPE and non-EKAPe species. *Frontiers in microbiology* 2019; 10: 2000. Doi: 10.3389/fmicb.2019.02000; PMID: 31543871.

**Source of Support:** The author(s) received no financial support for the research, authorship, and/or publication of this article.

**Conflict of Interest:** The author(s) declared no potential conflicts of interest with respect to the research, authorship, and/or publication of this article.

For any question relates to this article, please reach us at: [globalresearchonline@rediffmail.com](mailto:globalresearchonline@rediffmail.com)

New manuscripts for publication can be submitted at: [submit@globalresearchonline.net](mailto:submit@globalresearchonline.net) and [submit\\_ijpsrr@rediffmail.com](mailto:submit_ijpsrr@rediffmail.com)

